Allowable Delay Heuristic in Provision of Primary Frequency Reserve in Future Power Systems

Subir Majumder [ID], *Graduate Student Member, IEEE*, Ashish Prakash Agalgaonkar [ID], *Senior Member, IEEE*, Shrikrishna A. Khaparde [ID], *Senior Member, IEEE*, Sarath Perera [ID], *Senior Member, IEEE*, S. V. Kulkarni, *Fellow, IEEE*, and Philip Paul Ciufo [ID], *Senior Member, IEEE*

Abstract—With ever increasing penetration of inverter-interfaced generators and consequent reduction in available inertial reserve, traditional allowable delay in the provision of the primary frequency reserve will threaten the security of the future grids. However, droop control with fast-enough inertia-less generators can limit the post-contingency frequency excursion. To conform with the fast-enough reserve provision requirement in a reduced and varying-inertia system, an economical clearing of the reserve requires an allowable delay heuristic corresponding to the desired system frequency excursion characteristic; while alleviating the causality dilemma introduced by the unavailability of maximum delay heuristic itself before clearing. The proposed heuristic establishes a relationship among the system parameters, such as the aggregated system inertia, regulation factor, system frequency, desired frequency response, and allowable delay margin. The Padé approximation technique is utilized for deriving the transfer function of such a system, allowing calculation of the allowable delay with various damping ratios corresponding to the dominant poles. The impact of different Padé order on the determined heuristic is analyzed. The regulation factor of the generators is calculated based on the reserve bid volume to ensure proportional injection during contingencies. The impacts of regulation factor and associated delay on the frequency response are also studied.

Index Terms—Deadbeat response, golden search technique, low inertia power systems, padé approximation, primary frequency reserve, stability margin.

NOMENCLATURE

Sets:

$\mathbb{C}$	Set of complex numbers.
i	Index of reserve providing generators.
N	Set of all reserve providing generators.
$\mathbb{R}_{\geq 0}$	Set of non-negative real numbers.
t	Time, in s.
$\mathbb{Z}_{\geq 0}$	Set of non-negative integers.

Parameters:

a_k, b_k	The coefficients of the polynomial to obtain the rational approximation of the exponential function.
D	The aggregated damping factor provided by the loads and the damper winding of the synchronous generators in the system, if any, in pu-MW Hz^{-1}.
f_0	The nominal frequency of the power system, in Hz.
H	The reduced aggregated center of inertia (COI), inertia constant of the power system, in s.
$\mathcal{H}$	The aggregated COI inertia constant of the power system, in s.
m, n	Numerator and denominator rationalization order of the Padé approximant.
$\mathcal{M}$	Statistically calculated system load-generation imbalance, in MW.
R	Aggregated regulation provided by the reserve producing generators, in pu-MW^{-1} Hz.
S_B	System base power, in MVA.

Variables:

$G(\cdot)$	Transfer function representing the approximated retarded system.
$P_i^{inj}(t)$	Reserve injected from ith generator at time t, in MW.
$P^{inj}(t)$	Aggregated reserve injected at time t, in MW.
P_i^{bid}	Cleared bid for reserve provision from ith generator, in MW.
$\mathcal{Q}(\cdot)$	Frequency response of the ideal delay function.
R_i	Regulation provided by ith generator, in pu-MW^{-1} Hz.
R^1, R^2	Regulation provided by generators 1 and 2 respectively, in pu-MW^{-1} Hz.
$\mathcal{R}(\cdot)$	The Padé approximant.
$Re(\cdot)$	Real part of a complex number.
s	Complex frequency.
T_d	Delay in reserve provision, in s.
T_d^1, T_d^2	Delay in reserve provision from generator 1 and 2 respectively, in s.
T_d^{ms}	Delay in reserve provision corresponding to marginal stability condition calculated using Rekasius substitution, in s.

S. Majumder is with the Department of Energy Science and Engineering, Indian Institute of Technology Bombay, Mumbai 400076, India, and also with the Australian Power Quality & Reliability Centre, University of Wollongong, Wollongong, NSW 2522, Australia (e-mail: subirmajumder@iitb.ac.in).

A. P. Agalgaonkar and S. Perera are with the Australian Power Quality & Reliability Centre, University of Wollongong, Wollongong, NSW 2522, Australia (e-mail: ashish@uow.edu.au; sarath@uow.edu.au).

S. A. Khaparde and S. V. Kulkarni are with the Department of Electrical Engineering, Indian Institute of Technology Bombay, Mumbai 400076, India (e-mail: sak@ee.iitb.ac.in; svk@ee.iitb.ac.in).

P. P. Ciufo was with the Australian Power Quality & Reliability Centre, University of Wollongong, Wollongong, NSW 2522, Australia (e-mail: ciufo@uow.edu.au).

$u(t)$	Heaviside step function.
$\alpha_{deadbeat}$	Proportionality constant among the system parameters and estimated delay for deadbeat response.
$\alpha_{stability}$	Proportionality constant among the system parameters and estimated delay corresponding to marginal stability condition.
α_ζ	Proportionality constant among the system parameters and estimated delay in general.
$\Delta f(t)$	The deviation in the frequency of the power system at time t, in Hz.
$\Delta f(s)$	The deviation in the frequency of the power system in the frequency domain, in Hz.
$\Delta P(t)$	Load-generation imbalance at nominal operating frequency at time t, in MW.
$\Delta P(s)$	Load-generation imbalance at nominal operating frequency in the frequency domain, in MW.
$\Delta \mathcal{P}$	Signed load-generation imbalance, in MW.
ζ	Damping factor corresponding to the second-order equivalent of the retarded approximated system considering dominant poles.
ω_{cor}	Corner frequency of the equivalent second-order system, in rad/s.
ω_{crit}	The system frequency at which the gain threshold is reached, in rad/s.
ω_{cut}^{m,T_d}	The cut-off frequency of the Padé approximant, in rad/s.
ω_c, τ	Parameters of the Rekasius substitution, in rad/s, and s, respectively.

I. Introduction

A. Background

REDUCTION in the rotational inertia was first observed in the European Continental Synchronous Area [1], [2]. Corresponding low inertia system can mostly be attributed to high-penetration of the inverter-interfaced renewable energy (RE) resources, and rapid decommissioning of the traditional synchronous machine-based generators at the end of their lifetime [1]–[4]. Moreover, inverter-interfaced devices are expeditiously making inroads into power systems for better control with hardly any contributions to system inertia and load damping. Besides, the system damping provided by uncontrolled loads can be considered to be negligible compared to the regulation service provided by the primary frequency reserve (PFR) [5]. Under this scenario, to prevent the higher rate of change of frequency, provision of virtual inertia [2]–[4], [6], [7] from distributed resources becomes very much essential. However, although the inertia of the system is on the decline, residual inertia [2], [7] (from connected synchronous or induction machine based distributed generators, etc.) persists within the grid.

Power injections from converter-interfaced generating resources are primarily based on a centralized or decentralized estimate of the frequency [6], [8]. With the rapid deployment of the phasor measurement units and the availability of a wide area monitoring system, an additional latency concerning the unavailability of non-local signals is reduced. Although it is possible to obtain coherent measurements of the whole power
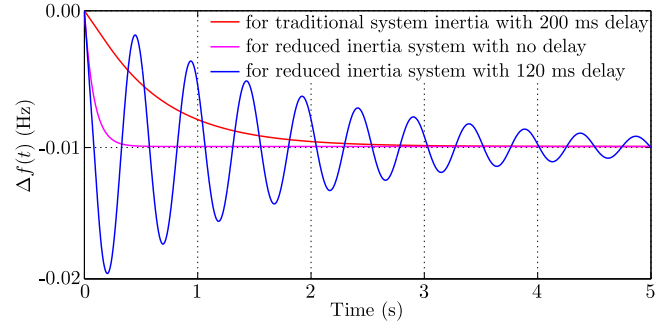

Fig. 1. Dynamic frequency responses of the retarded single machine load bus system wherein inertia is reduced to 10% of typical system inertia.

TABLE I
SYSTEM PARAMETERS

Parameter	Variable	Value
Inertia of Traditional Power System	$\mathcal{H}$	100 s
Base Power	S_B	100 MVA
Reduced Inertia of the Power System	H	10% of $\mathcal{H}$
Load Damping (Reduced)	D	0.03 pu-MW/Hz
System Nominal Frequency	f_0	60 Hz
Emulated Speed Governor Regulation	R	0.25 Hz/pu-MW

system in almost real-time, the cost and associated complexities restrict their use in the traditional power system. In contrast, existing communication channels increase the latency in the frequency measurement [9] (the typical total latency of the communication channel is 40–140 ms [8], [10]). Moreover, delays in injection from fast-acting storage devices are also non-zero, and are limited by their response time [8].

Traditionally, during an emergency condition within a power system, the inertia of the system is large enough to maintain the stability of the system for the first few seconds [11]. However, if all other parameters are held constant, increasing the delay in the PFR provision, calculated based on frequency imbalance, monotonically brings a system into small-signal instability [12]. Therefore, the delayed provision of the reserve becomes prominent in a low inertia power system. Fig. 1 shows a comparative analysis of the frequency response of a retarded system, where the system inertia reduces to 10% of the traditional high inertia system. In contrast, the PFR provision in a traditional power system (refer to the system shown in Table I) needs to be fully available within a time range of 5–10 s [11], [13].

B. Literature Review

An extensive literature is available to study the impact of delayed reserve provision on the response of the power system. Typically, the maximum allowable delay estimation methods tend to be exact and only suitable for determining the marginal stability condition of the system. In this regard, [14], [15] uses Rekasius substitution, [13], [16] removes the transcendental part without losing exactness, and [17] relies on the stability criterion determined from matrix pencil solutions. A computationally tractable algorithm is proposed in [18]. Although linearized substitutions presented in [13]–[16] are exact, they can only be used to find out the marginal stability condition.

A pure delay function introduces infinitely many roots in the characteristic equation. However, based on the location of the poles and the associated residues, only specific poles of the transcendental system have a significant effect following a disturbance. In this regard, Chebyshev's method has successfully been applied to determine the impact of delays on small-signal stability condition [19].

The correlation among the delay margin and the controller gain is investigated in [20]. A Jordan-Taylor-Schur approach to obtain allowable maximum time delay that ensures marginal stability of the system has been discussed in [21]. Calculation of delay margin that ensures scalability with increasing size of the system has been addressed in [22]. The allowable delay is iteratively calculated in [23] by identifying crossing frequencies through a sweeping test.

Use of linearization techniques to express a retarded system are also abundant. The Padé approximation is a widely used rational approximation which tends to accurately represent the frequency response of latency [24]–[28]. The stability analysis of a large power system with inclusion of multiple delays is carried out in [27], and delays are modeled using both Chebyshev and Padé approximations for comparison. In [29], the communication delay is modeled using the first-order Padé approximation to analyze the system stability. A linear matrix inequality approach to assess the stability criterion of load frequency control is presented in [30].

C. Problem Statement

Fast enough PFR provision alone can stabilize a system following a contingency. The provision of speed-governor like response from inverter-interfaced generators necessitates measurement and communication of frequency deviations to each of the reserve providing generators. Policymakers can also attract participation through alleviating strict reserve dispatch rules, and reserve providers will be economically cleared in the electricity market. In this paradigm, however, along with traditional price-quantity and ramp-rate information, the reserve provisioning bidders would also have to provide information about the speed of the reserve provision. Because of the varying residual inertia within the grid, the allowable delay would also vary. And therefore, the allowable delay in the PFR dispatch needs to be periodically reviewed. Additionally, contrary to the definition provided in [14], the system operator need not solely be interested in the marginal stability condition of the system. Moreover, the delay needs to conform to the worst-case frequency response imposed by the system operator.

The literature review indicates that computed maximum allowable delay depends on various system parameters, such as network topology, locations of the reserve providing generators, characteristics of these generators, etc. However, in the future reserve market, if not all generators that participate are cleared (different markets clear reserves differently, refer to [31]), the maximum allowable delay in the PFR provision determined by the set of all the participating reserve providers, will be erroneous. This will lead the system operator into causality dilemma, wherein the determination of the allowable delay of the power system requires clearing of all the reserve providing generators, while the allowable delay estimate itself is required to clear them. Therefore, the existing computational techniques are ineffective to obtain the allowable delay criterion before the generators are cleared in the electricity market. The availability of an approximate estimate of the allowable delay will help the market operator to clear successful PFR providing entities while ensuring a worst-case frequency response demanded by the system operator.

Once the market operator selects suitable set of generators, the system operator may use a detailed model of generators and the network to determine the feasibility of the economically efficient PFR. If the initially selected efficient set of bidders cannot ensure the desired frequency response of the system; the system operator can identify the generator(s) leading to the unacceptable condition, and opt for economically next best suitable generator. Therefore, the primary objective of this paper is to obtain a computationally inexpensive heuristic of allowable system delay, which is independent of the location and characteristics of reserve provisioning generators.

D. Contributions

The contributions of this paper are threefold:

a) A simple heuristic to calculate the allowable delay in an approximated power system is needed. Although the presented heuristic lacks exactness, it is not limited to finding the latency corresponding to the marginal stability condition. Furthermore, the proposed system-independent heuristic will help the market operator to clear successful reserve providing generators. To validate the proposed heuristic, the allowable latency calculated corresponding to the marginal stability condition is compared with the exact solution obtained from the Rekasius substitution.

b) Accuracy of the sought Padé approximation is high in the low-frequency region of the frequency response of the delay, defined by a cut-off frequency. However, given a certain Padé order, if the gain of the system falls below a certain threshold at the introduced cut-off frequency (which is also called as the gain threshold), and is declining, it can be said that the associated Padé order, can successfully represent the delayed system. The impact of various Padé orders and gain threshold on the proposed heuristic is also presented.

c) Because, the regulation factor of the individual generators is determined only after all the generators are cleared based on the proposed maximum allowable delay criterion, individual regulation factors and associated delays are not directly accounted while calculating the proposed heuristic. However, it is unrealistic that all the reserve providing generators will simultaneously inject reserve into the grid and therefore, the impact of regulation factors and delays on the frequency response of the system have also been studied through numerical time-domain simulation. Additionally, calculation of the regulation factor of each of the reserve providing generators based on its bid volume is also presented.
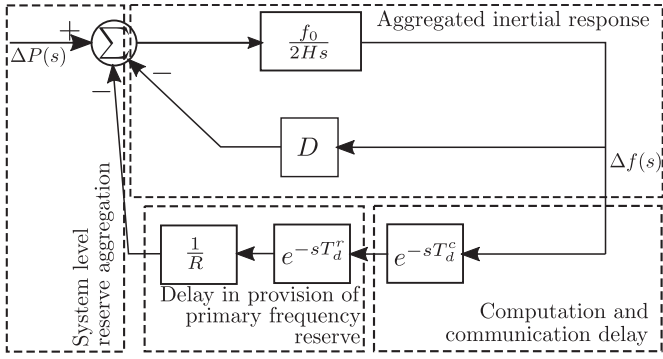
Fig. 2. Derived block diagram for analyzing the frequency dynamics of low-inertia system.

E. Paper Organization

The remainder of the paper is organized as follows. Provision of reserve in a low-inertia, retarded single machine load bus system has been described in Section II. Padé approximation for representing the delayed reserve provision, has been described in Section III. Analytical calculation and its validation using a numerical example to show the efficacy of the heuristic is shown in Section III. Sections IV and V constitute comments and conclusion, respectively.

II. PROVISION OF RESERVE IN A LOW INERTIA SYSTEM

In recent literature, along with distributed generators [3], [4], [32], storage devices [1]–[4], [33], [34] and electric vehicles [29], aggregated controllable loads [4], [28], [35] are also being treated as reserve providing generators. Based on the response time, controllable loads can participate in primary [28], [36] or secondary [35] frequency reserve in the future grid. However, the aggregation of loads and their control for reserve provision is limited by the complexity of the communication interface between the central controller and small loads [36].

The following additional assumptions are made: (i) finite inertia exists within the grid, (ii) frequency imbalance with finite system inertia can be measured, (iii) residual inertia does not participate in PFR provision, (iv) the control signal to inverter-interfaced distributed generators can be sent so that they respond to any frequency deviation, (v) injection from inverter-interfaced PFR providers is proportional to both frequency deviation of the system from normal frequency condition and allocated droop, and (vi) injection of reserve is delayed. The derived block diagram of an inverter-interfaced low-inertia system, based on these assumptions, is shown in Fig. 2.

It is imminent that the block diagram is obtained by neglecting local electromechanical transients and oscillation modes. Suppose, T_d^c is detection and communication latency as discussed earlier, and T_d^r is the internal response time of the inverter-interfaced reserve providing entities (considered to be an ideal delay for simplicity). This model can be further simplified by considering that all reserve providing resources dispatch simultaneously after an ideal delay of $T_d (= T_d^c + T_d^r)$. Aggregated system inertia and damping are given by H and D respectively, and Δf is the center of inertia (COI) frequency deviations from the nominal frequency, f_0, of the power system. $\Delta P(t)$ is a

typical generation-load mismatch, R_i are the regulation factors of each of the reserve providing inverter-interfaced generators, and $R \left(= (\sum_{\forall i} 1/R_i)^{-1}\right)$ is the aggregated regulation factor of the system. As indicated, a simplified model of the power system is considered in this paper. Based on elementary principles of dynamics, frequency deviations around the nominal operating frequency for the low-inertia, primarily inverter-interfaced system can be given by the retarded aggregated swing equation,

$$\frac{2H}{f_0}\frac{d\Delta f(t)}{dt} + D\Delta f(t) + \sum_{\forall i}\frac{1}{R_i}\Delta f(t - T_d)$$
$$= \Delta P(t) = \Delta \mathcal{P}u(t) \qquad (1)$$

The impact of the ramp rate on the system stability is not considered in this paper considering that the internal response time of reserve provisioning entities (such as batteries, flywheels, supercapacitors) can be very fast [37]. Ignoring the delayed power injection, the relationship among the regulation factors $(R_1, R_2 \dots R_N)$ of distributed resources and associated power injections $(\Delta P_1^{inj}, \Delta P_2^{inj} \dots \Delta P_N^{inj})$ for the droop control will be given by:

$$R_1\Delta P_1^{inj}(t) = R_2\Delta P_2^{inj}(t) = \cdots = R_N\Delta P_N^{inj}(t) = \Delta f(t) \qquad (2)$$

Regulation settings are hypothetical quantities. Solving (1), assuming $H \to 0$, and using the assumption, $RD \approx 0$, one obtains,

$$\Delta f(t) \approx R\Delta \mathcal{P}u(t) \qquad (3)$$

The total power injected into the grid in steady-state will be, $P^{inj}(t) \approx \frac{\Delta f(t)}{R} \approx \Delta \mathcal{P}u(t)$. Therefore, in a system with very low inertia and very low inherent damping, power injection from the reserve providing entities will be "instantaneous," and injection at steady-state will be approximately equal to the total power imbalance. However, a high rate of change of frequency similar to that in Fig. 1 will be observable (the direction of the jump will be based on the sign of $\Delta \mathcal{P}$).

It is to be noted that, frequency response in a power system will be driven by simultaneous injections from all entities cleared to provide the PFR. Therefore, if a generator i ($i \in N$, with N being the set of all cleared reserve providing generators) is assigned with the regulation of R_i, with $\Delta f(t)$ as the system frequency deviation, its power injection into the grid can be obtained as:

$$\Delta \mathcal{P}u(t) = \Delta f(t)\sum_{i \in N}\frac{1}{R_i} = \sum_{i \in N}P_i^{inj}(t) \qquad (4)$$

From (1), (3) and (4), the injection from each generator can be given by $P_i^{inj}(t) = \frac{R}{R_i}\Delta P(t)$. Suppose, the generator i bids with P_i^{bid} as PFR provision, and the system operator wants to select R as the aggregated regulation factor while willing to limit a maximum of statistically calculated power imbalance $\mathcal{M}$, then the regulation factor of each of the PFR providing generators, R_i, can be given by,

$$R_i = \frac{R}{P_i^{bid}}\mathcal{M} \qquad (5)$$

Equation (5) above would ensure that given a contingency, each of the generators injects in proportion to its bid volume
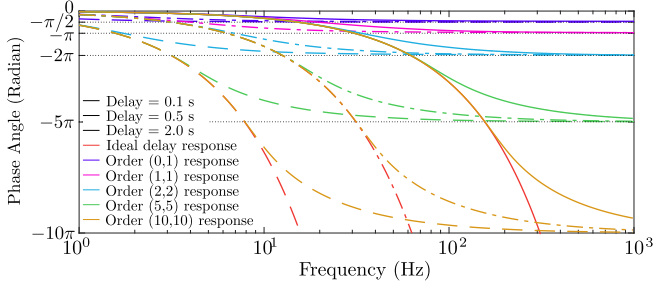
4

Fig. 3. Impact of rational approximations on frequency responses of the ideal delay.

and the power imbalance. Given that the frequency droop is hypothetical, smaller R will lead to the desirable lowered steady-state frequency error. In the following sections, the impact of R on the allowable delay of the system is studied.

III. REQUISITE PADÉ APPROXIMATION OF DELAYS

A rational function can be used to approximate the frequency response of the delay function by ignoring insignificant eigenvalues associated with the higher-order part of the ideal frequency response. Besides, when the delayed system is causal and the delay is not large, the Padé approximation can be competent [24], [25]. Let, $\mathcal{R}(m, n, s, T_d)$ represents the rational function approximation with its numerator and denominator of order m and n respectively. Here, s is the complex frequency, used as a variable in Laplace transformation, and, T_d is the time delay of the system. The polynomial function representing the approximation can be given by [25], [26],

$$e^{-sT_d} \approx \mathcal{R}(m, n, s, T_d) = \frac{\sum_{k=0}^{m}(-1)^k a_k(sT_d)^k}{\sum_{k=0}^{n} b_k(sT_d)^k} \quad (6)$$

Representation accuracy increases with an increasing order of approximation. However, because of the precision arithmetic used in modern computers, the order of the the rational approximation is often limited. Additionally, the benefit of using higher-order Padé approximations has a diminishing return [28]. Now, if $m = n$, the amplitude of the response of both delay and its rational approximant is unity [26]. Therefore, similar numerator and denominator polynomial order have been considered in this paper. The frequency response of the ideal delay and the associated rational approximation with Padé order m (both numerator and denominator polynomial order) is given in (7) and (8) and it is depicted in Fig. 3,

$$\mathcal{Q}(\omega) = e^{-j\omega T_d} \quad (7)$$

$$\mathcal{R}(m, \omega, T_d) = \frac{\sum_{k=0}^{m}(-1)^k a_k(j\omega T_d)^k}{\sum_{k=0}^{m} b_k(j\omega T_d)^k} \quad (8)$$

Frequency response in Fig. 3 indicates that the phase response of the Padé approximant is only valid for the low-frequency region while saturating at the phase of $-m\pi$. Therefore, the cut-off frequency is defined by the frequency at which the phase response of the ideal delay function is equal to the saturated phase response of the rational approximant. This definition

is accounted, because, beyond the concerned frequency, the phase response of the approximant will never reach the phase response of the ideal delay. Such limitation captured by the cut-off frequency is expected to help us in identifying a suitable approximation of the retarded transfer function. For the mth order Padé approximant, the cut-off frequency will be,

$$\omega_{cut}^{m,T_d} = \frac{m\pi}{T_d} \quad (9)$$

Fig. 3 also shows that as the considered delay T_d increases, for a given order of approximant, the cut-off frequency decreases.

Therefore, for successful representation of the delay function, the critical frequency of the approximated system must be smaller than the cut-off frequency determined by the Padé approximant. The critical frequency of the system can be defined by the frequency beyond which the gain of the overall system will be negligible enough to account for. This way, the approximation will have negligible impact on the response of the system. Mathematically,

$$\omega_{crit} \leq \omega_{cut}^{m,T_d} \quad (10)$$

It is observable that ω_{crit} is dependent upon the gain threshold (pre-decided gain beyond which the gain of the system is too small to consider), and therefore, decreasing the gain threshold would increase the approximation order.

IV. IMPACT OF DELAY

Given the rational approximation, if system poles $\lambda_x \in \mathbb{C}$ of order y_x correspond to a residue of $r_x \in \mathbb{C}$, then the overall transfer function of the approximated system, $G(s)$, can be written as,

$$G(s) = \sum_{\forall x, \forall y} \frac{r_x}{(s - \lambda_x)^{y_x}} \quad (11)$$

It is well known that the relative dominance of closed-loop poles essentially characterizes the stability of the system. The system is inherently unstable, if $Re(\lambda_x)$ is positive, or, there exist repeated poles with $Re(\lambda_x)$ equals zero. Otherwise, if the ratio of $Re(\lambda_x)$ of any two pole pairs exceed five, then the pole with larger $Re(\lambda_x)$ will be dominant [38]. If the ratio is lowered, then the poles with higher $\frac{|r_x|}{|Re(\lambda_x)|}$ will correspond to the dominant pole [39]. The dominant pole (or, pole pair) considered in this paper is the one with significant impact on the system response.

Fig. 4 shows the movement of the dominant pole for a reduced inertia system of Table I with the delay, T_d, and various approximation orders.

From Fig. 4, it can be observed that for the (0,1) approximation, the system is stable independent of any delay. The analytical reason behind these observations is presented later in this paper. It is also notable that, for a given delay, the location of the eigenvalue converges with increasing order of the approximation. T_d is varied until 500 ms in this case study.
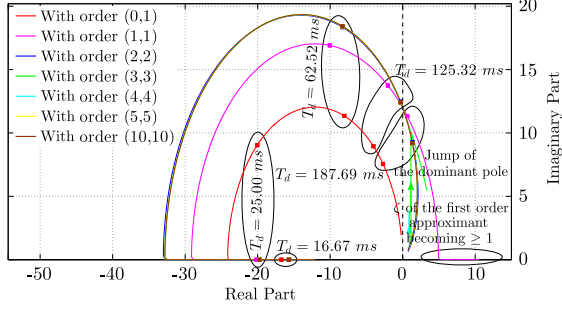
5

Fig. 4. Trace of dominant poles of the system with increasing delay in the reserve provision.

A. Calculation of Delay for Deadbeat and Marginal Stability

Given an order of approximation and $\Delta P(s) = -\frac{\Delta \mathcal{P}}{s}$, using the final value theorem on (1):

$$\lim_{s \to 0} s\Delta f(s) = -\lim_{s \to 0} \frac{s\frac{\Delta \mathcal{P}}{s}}{\frac{2Hs}{f_0} + D + \frac{\mathcal{R}(m,n,s,T_d)}{R}} = -\frac{\Delta \mathcal{P}}{D + \frac{1}{R}} \quad (12)$$

Using the final value theorem on the system with pure delay:

$$\lim_{s \to 0} s\Delta f(s) = -\lim_{s \to 0} \frac{s\frac{\Delta \mathcal{P}}{s}}{\frac{2Hs}{f_0} + D + \frac{e^{-sT_d}}{R}} = -\frac{\Delta \mathcal{P}}{D + \frac{1}{R}} \quad (13)$$

Steady-state solutions obtained from (12) and (13) are not applicable for an unstable system. However, if a given system is stable and numerical instability can be avoided, the approximant exactly calculates the final value. Although a higher-order rational approximation generates a better solution, algebraic calculation of dominant poles can be realized for approximation orders of (0,1), and (1,1), and the numerical calculation needs to be sought for higher-order approximations. Therefore, the locations of the poles or the pole pairs are calculated for the deadbeat and the marginally stable condition of the approximated system as described further.

1) With Rationalization Order (0,1): Substituting (0,1) Padé approximant in (1), the following relation is obtained,

$$\frac{2Hs}{f_0}\Delta f(s) + D\Delta f(s) + \frac{\Delta f(s)}{R(sT_d + 1)} = \Delta P(s) \quad (14)$$

If, $H, f_0, D, R, T_d \neq 0$, the following transfer function is obtained,

$$\frac{\Delta f(s)}{\Delta P(s)} = \frac{f_0 R(sT_d + 1)}{2HRT_d s^2 + (2H + Df_0T_d)Rs + (RD+1)f_0} \quad (15)$$

Now, because $2HRT_d \neq 0$, we get,

$$\frac{\Delta f(s)}{\Delta P(s)} = \frac{\frac{f_0}{2HT_d}(sT_d + 1)}{s^2 + \frac{2H + Df_0T_d}{2HT_d}s + \frac{(RD+1)f_0}{2HRT_d}} \quad (16)$$

It is imminent that there exists no $T_d \geq 0$ such that the poles of (16) lie on the imaginary axis. And therefore, based on the (0,1) approximation, the system is inherently stable for $T_d \in [0, \infty)$, as it is observed in Fig. 4.

Since the system is inherently stable, one can calculate ζ^2 corresponding to the dominant pole. The damping factor of the dominant poles of (16) can be calculated as,

$$\zeta^2 = \frac{R}{8}\frac{(2H + Df_0T_d)^2}{Hf_0T_d(1 + RD)} \quad (17)$$

The system response will not overshoot, if

$$\zeta^2 = \frac{R}{8}\frac{(2H + Df_0T_d)^2}{Hf_0T_d(1 + RD)} \geq 1 \quad (18)$$

With simple algebraic manipulation, the following relationship is obtained,

$$D^2 f_0{}^2 T_d^2 - 4Hf_0\left(D + \frac{2}{R}\right)T_d + 4H^2 \geq 0 \quad (19)$$

The inequality in (19) holds, if,

$$T_d \geqslant \frac{2H}{D^2 f_0 R}\left(2 + RD + 2\sqrt{RD + 1}\right) \quad (20a)$$

$$T_d \leqslant \frac{2H}{D^2 f_0 R}\left(2 + RD - 2\sqrt{RD + 1}\right) \quad (20b)$$

Inequality in (20a) can be ignored for being infeasible (note that if both $RD \to 0$, and $R, D \neq 0$ are true, then, $\frac{2HR^2}{f_0}\lim_{RD \to 0}\frac{(2+RD+2\sqrt{RD+1})}{(RD)^2}$ will be undefined). With Taylor series approximation, (20b) reduces to,

$$T_d \leqslant \frac{2H}{D^2 f_0 R}\frac{R^2 D^2}{4} = \frac{HR}{2f_0} \quad (21)$$

It is notable that $RD \in \mathbb{R}_{\geq 0}$, and the condition $RD \ll 1$ is true even in a traditional power system [5]. Therefore, with the rationalization order (0,1), if $T_d \leqslant \frac{HR}{2f_0}$, the system ζ will be ≥ 1.

For an arbitrarily selected ζ ($\in [0,1]$), the allowable delay will be,

$$T_d \leqslant \frac{1}{2\zeta^2}\frac{HR}{f_0} \quad (22)$$

2) With Rationalization Order (1,1): Similar to the (0,1) approximation, applying Laplace transform to (1), the following relationship is obtained,

$$\frac{2Hs}{f_0}\Delta f(s) + D\Delta f(s) + \frac{\Delta f(s)}{R}\frac{-sT_d + 2}{sT_d + 2} = \Delta P(s) \quad (23)$$

Also, if $H, f_0, D, R, T_d \neq 0$, then, we obtain

$$\frac{\Delta f(s)}{\Delta P} =$$

$$\frac{f_0 R(sT_d + 2)}{2HRT_d s^2 + (4RH + RDf_0T_d - f_0T_d)s + 2(RD+1)f_0} \quad (24)$$

From (24), $T_d \in [0, \infty)$, the condition when the poles of (16) lie on the imaginary axis:

$$T_d = \frac{4RH}{f_0(1 - RD)} \approx \frac{4RH}{f_0}(\text{for } RD \to 0) \quad (25)$$

And therefore, based on the (1,1) approximation, if $T_d \leq \frac{4RH}{f_0}$, the system will be small-signal stable.

6

Given that the system is stable, one can calculate ζ^2 corresponding to the dominant poles. The damping factor of the dominant poles in (24) can be calculated as,

$$\zeta^2 = \frac{1}{16} \frac{(RDT_d f_0 + 4RH - T_d f_0)^2}{RH f_0 T_d (1 + RD)} \tag{26}$$

For an over-damped condition,

$$\frac{1}{16} \frac{(RDT_d f_0 + 4RH - T_d f_0)^2}{RH f_0 T_d (1 + RD)} \geqslant 1 \tag{27}$$

The inequality in (27) holds if,

$$T_d \geqslant \frac{4RH}{f_0} \frac{\left(3 + RD + 2\sqrt{2}\sqrt{RD + 1}\right)}{(1 - RD)^2} \tag{28a}$$

$$T_d \leqslant \frac{4RH}{f_0} \frac{\left(3 + RD - 2\sqrt{2}\sqrt{RD + 1}\right)}{(1 - RD)^2} \tag{28b}$$

For a system with $\zeta \geqslant 1$, the system delay, T_d, can be obtained from (28b):

$$T_d \leqslant \frac{4RH}{f_0} \left(3 - 2\sqrt{2}\right) \tag{29}$$

However, given that $RD \to 0$, using (28a), for $\zeta \geqslant 1$, we obtain $T_d \geq \left(3 + 2\sqrt{2}\right) \frac{4RH}{f_0}$. But, owing to (25), the system is unstable for $T_d > \frac{4RH}{f_0}$. This false positive behaviour can be observed in Fig. 4. Therefore, with the rationalization order $(1,1)$, if $T_d \leqslant \frac{4RH}{f_0} \left(3 - 2\sqrt{2}\right)$, the system damping factor will be ≥ 1.

For an arbitrarily selected $\zeta\,(\in [0, 1])$, the allowable delay will be:

$$T_d \leqslant 4\left\{(1 + 2\zeta^2) - \sqrt{(1 + 2\zeta^2)^2 - 1}\right\} \frac{HR}{f_0} \tag{30}$$

3) Numerical Verification: Because the delay estimates obtained from the $(0,1)$ and $(1,1)$ approximants are imperfect, to obtain the true allowable delay requirements, if $H, f_0, D, R, T_d \neq 0$, and $RD \to 0$, the following proposition can be made:

Proposition: The allowable delay, calculated based on the dominant poles, and given by $T_d = \alpha_{\text{deadbeat}}(m) \frac{HR}{f_0}$, will result into a deadbeat response of the system. If the allowable delay is $T_d = \alpha_{\text{stability}}(m) \frac{HR}{f_0}$, then the response of the system is marginally stable. α_{deadbeat} and $\alpha_{\text{stability}}$ are non-dimensional proportionality constants that depend on the Padé order.

As already indicated, numerical calculations are resorted to for the higher-order system. The golden search technique has been used to find the corresponding delay for the given parameters.

Fig. 5 verifies that the delay with the deadbeat response is proportional to parameters H and R, while it is inversely proportional to f_0 for the system presented in Table I. Because of the application of the Padé approximation, a lower-order approximation is found out to be an underestimate. Allowable delay converges with higher-order approximations. As expected, the estimated delay is independent of the parameter D (for a typical value). Similar characteristics are also observed for systems with different parameters, but details are omitted for brevity.
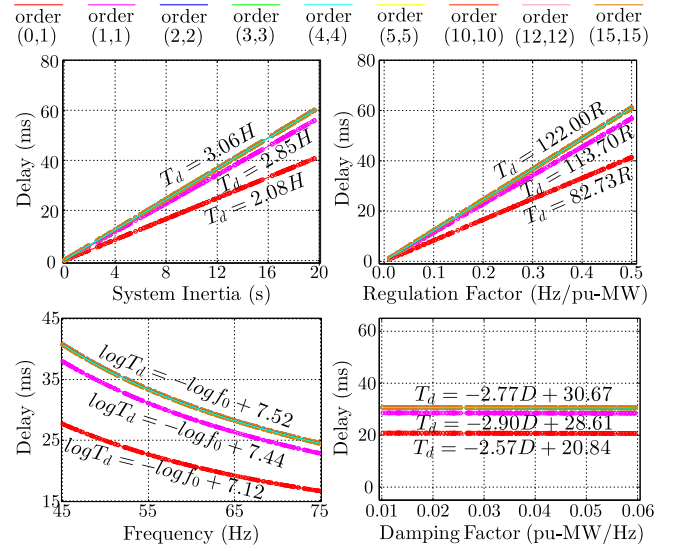

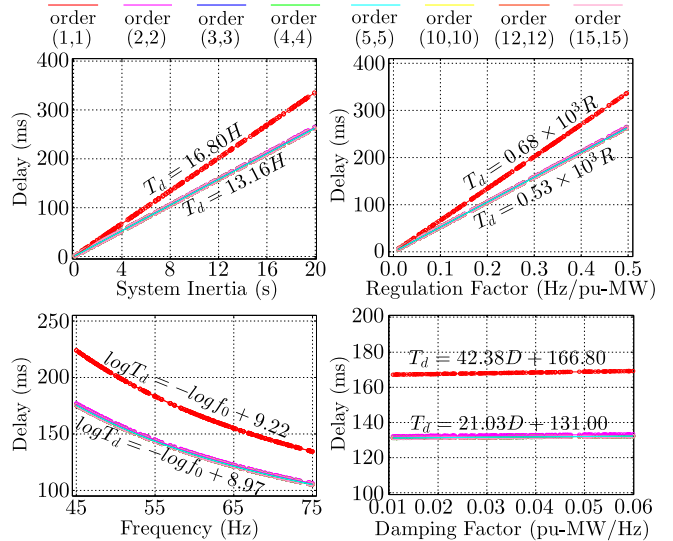Fig. 5. Impact of rational approximation of delay for the deadbeat response.

Fig. 6. Impact of rational approximation of delay for the marginally stable condition.

Fig. 6 also verifies that the delay corresponding to the marginal stability condition is proportional to H and R, while it is inversely proportional to f_0. Since $RD \to 0$, as shown, the factor $(1 - RD)^{-1}$ converges to $(1 + RD)$. Therefore, the impact of the parameter RD is deemed negligible in the calculation of the allowable delay. Similar system responses are also observed for systems with different parameters but are not included for brevity.

Fig. 7 depicts the existence of a one-to-one relationship between ζ and α (also can be depicted as α_ζ) of the system of Table I. The characteristic curves satisfy (22) and (30). Artifacts with longer delays are ignored in this graph. Furthermore, the analysis also shows that the relationship between ζ and α is applicable for a different system with different H, D and R, but, with $RD \to 0$ with reasonable accuracy.
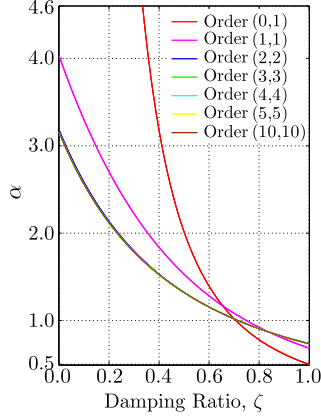
Fig. 7. ζ versus α graph for an equivalent second-order system with $RD \to 0$.
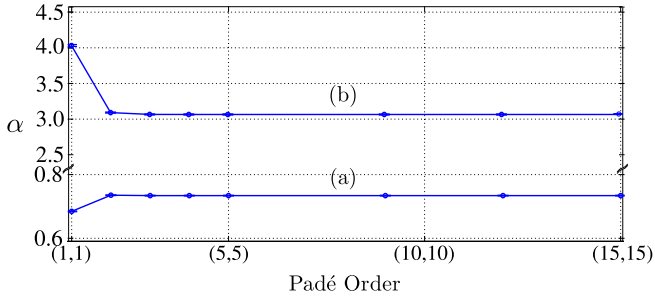

Fig. 8. Impact of the rational approximation on the delay heuristic: (a) for critically damped response, (b) for marginally stable response.

Fig. 8 shows that α_{deadbeat} and $\alpha_{\text{stability}}$ converge with a higher-order Padé approximation with negligible coefficient of variation. The corresponding coefficients are calculated as $\alpha_{\text{deadbeat}} = 0.73$ and $\alpha_{\text{stability}} = 3.16$.

4) Analytical Verification for Marginally Stable System: Ideally, the Rekasius substitution, defined as the following, generates the exact condition for marginal stability [14], [15]:

$$e^{-sT_d} = \left\{ \frac{1-\tau s}{1+\tau s} \left| T_d = \min_{\forall k} \left[\frac{2}{\omega_c} \tan^{-1}(\omega_c \tau) \pm k\pi, \right. \right. \right.$$
$$\left. \left. \left. \forall k \in \mathbb{Z}_{\geq 0} \right] ; \quad s \in \mathbb{C} \right\} \right.$$
(31)

Using the method presented in [14], for the given problem, we obtain,

$$\omega_c = \frac{f_0}{2HR}\sqrt{1 - R^2 D^2}; \quad \tau = \frac{2HR}{f_0(1 - RD)}$$
(32)

The delay margin, T_d^{ms}, can be calculated as,

$$T_d^{ms} = \inf_k \left[\frac{4HR}{f_0\sqrt{1-R^2D^2}} \tan^{-1}\left(\sqrt{\frac{1+RD}{1-RD}}\right) \pm k\pi, \right.$$
$$\left. \forall k \in \mathbb{Z}_{\geq 0} \right]$$
(33)

As considered before, assuming $RD \to 0$, $\tan^{-1}(\sqrt{\frac{1+RD}{1-RD}}) \to \frac{\pi}{4}$,

$$T_d^{ms} = \frac{\pi HR}{f_0}$$
(34)

Padé Order	T_d (ms)	ω_{cor} (rad/s)	ω_{cut}^{m,T_d} (rad/s)	Gain at ω_{cut}^{m,T_d}	Decreasing Gain ?
1	28.5	0.7	110.2	-30.4 dB	Yes
2	30.6	1.4	205.0	-37.2 dB	Yes
3	30.6	1.0	308.1	-40.1 dB	Yes
4	30.6	1.0	410.8	-42.7 dB	Yes

The coefficient obtained in (34) closely matches with the numerically calculated $\alpha_{\text{stability}}$ value of 3.16. However, because of the presence of zeros in (24), the calculated α_{deadbeat} value will be an overestimate.

5) Complexity: From the proposition, it is to be noted that once H, R and f_0 of the aggregated system are known, using Fig. 7, the allowable delay can be calculated with the complexity of $O(1)$. However, this computational inexpensiveness is achieved at the expense of considering the simplified model of the system to alleviate the causality dilemma faced by the market operator. Nevertheless, the proposed heuristic should not be used as a substitute for the detailed complex model to analyze the stability of the power system under study.

B. Impact of the Gain Threshold on the Padé Order

Although Figs. 5, 6, 7 and 8 indicate that the approximation order of more than two will usually generate good approximation, it is also of interest to determine the impact of the gain threshold on the approximation order.

If $m = n$, for the given system, the order of the numerator polynomial is less than the order of the denomnator polynomial. And therefore, the gain of the system at $\omega \to \infty$ converges to zero and thereby mimics low-pass response. A Padé order is feasible if the corner frequency, ω_{cor}, corresponding to the dominant pole (or pole pair) is lower than the cut-off frequency, ω_{cut}^{m,T_d}. If the condition is true, we calculate the gain at the frequency ω_{cut}^{m,T_d}. Typically, it is well known that when the gain of the system is attenuated to 70.7% ($1/\sqrt{2} \times 100\%$), and the overall gain of the system is monotonically decreasing, the impact of the system response beyond the frequency corresponding to 70.7% of the DC gain will be insignificant. Therefore, the Padé order, at which, the gain is below -3.1 dB of the DC gain of the system at, ω_{cut}^{m,T_d}, and beyond, ω_{cut}^{m,T_d}, the gain is monotonically decreasing, will be a good enough approximation of the considered system.

For the system parameters presented in Table I, the DC gain, $20\log_{10}|G(0)|$, is equal to -12.1 dB. The delay obtained from the dominant pole analysis, the corner-frequency corresponding to the dominant poles, ω_{cut}^{m,T_d}, the gain of the system at ω_{cut}^{m,T_d}, and the condition that the gain is decreasing beyond ω_{cut}^{m,T_d}, corresponding to the deadbeat response and the marginal small-signal stability condition are presented in Tables II and III, respectively.

Corresponding to the deadbeat response of the system, for all possible Padé orders considered, $\omega_{cor} < \omega_{cut}^{m,T_d}$, the gain at ω_{cut}^{m,T_d} falls below -15.1 dB, and the gain is monotonically decreasing at ω_{cut}^{m,T_d}. Therefore, as can be seen in Table II,

TABLE III
PADÉ ORDER AND ASSOCIATED DELAY FOR THE MARGINALLY STABLE SYSTEM

Padé Order	T_d (ms)	ω_{cor} (rad/s)	ω_{cut}^{m,T_d} (rad/s)	Gain at ω_{cut}^{m,T_d}	Decreasing Gain ?
1	168.0	12.0	18.7	-9.8 dB	Yes
2	132.6	12.0	47.4	-25.9 dB	Yes
3	131.6	12.0	71.6	-26.9 dB	Yes
4	131.6	12.0	95.5	-30.0 dB	Yes

Fig. 9. Dynamic responses of the power system to a sudden power imbalance.

all possible Padé orders will provide us with a feasible delay margin. It is also to be noted that the use of a higher-order approximation compared to the first-order approximation will result in improvement of the delay margin only by 7.4%.

Corresponding to the marginal stability condition of the system, for all Padé orders considered, $\omega_{cor} < \omega_{cut}^{m,T_d}$. However, with the Padé order of unity, the gain at ω_{cut}^{m,T_d} is higher compared to the DC gain and is therefore not suitable for the calculation of delay margin. For all other higher approximation orders, the gain at ω_{cut}^{m,T_d} falls below -15.1 dB, and these approximations will provide feasible delay margin.

C. Time Domain Response of the Power System With Multiple Delays

α_ζ in the derived heuristic, $T_d = \alpha_\zeta \frac{HR}{f_0}$, is the converged non-dimensional proportionality constant corresponding to the damping factor, ζ, of the power system. However, in the future power system with multiple small reserve providing generators, the delay in the provision of the reserve from the different generators may not be consistent. And the assumption that the reserve is available from all the generators after a constant delay may not be practicable. Furthermore, as it has been observed, both delays and regulation factors have a direct impact on the dynamic response of the power system.

For analyzing the impact of multiple delays, two generators with regulation factors, R^1 and R^2 of 0.750 and 0.375 Hz/pu-MW, respectively, are considered to be providing reserve. If both generators simultaneously inject reserve, the allowable delay for the deadbeat response will be 30.4 ms, and for the marginal stability condition it will be 131.7 ms. If the inertia of the low-inertia system increases by 50% to 15 s, the corresponding allowable delay for the deadbeat and the marginal stability condition will be 45.6 ms and 197.5 ms respectively. Given these extremities, the dynamic response of the power system with different regulation factors and associated delays can be examined through Fig. 9.

Higher initial rate of change of frequency with increased system inertia, similar to that in Fig. 1 can also be observed. Because the delay is directly proportional, while the bid volume being inversely proportional to the regulation factor, faster provision of the reserve from the generator with larger bid volume would ensure stability even if the delay in the provision of the reserve from generators with a higher regulation factor is more than (or, close to) allowable. Furthermore, the system response is always better than that of the dispatched generator with worst-case delay.
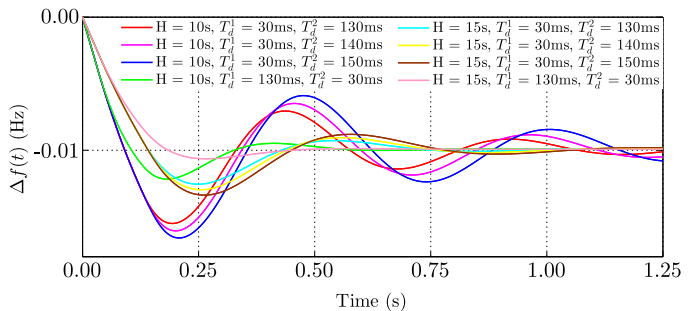
Notably, the network is assumed to be highly meshed in the above analysis. If the interconnected network divides into multiple areas following a disturbance, the synchronizing coefficient of tie-lines would also impact the allowable delay heuristic.

V. FURTHER COMMENTS

It has been noted that the system regulation factor is a fictitious quantity. Increasing this factor while maintaining sufficient system inertia will effectively increase the allowable delay margin for a given frequency response, but at the expense of increased steady-state error. Therefore, an optimal selection of the overall regulation factor is essential.

One of the assumptions in this paper is that the provision of the reserve is not tied to the speed-governor response. Instead, inverter-interfaced renewable energy generators or storage devices provide inertial reserve in response to the communicated frequency imbalance. While the discussed allowable latency can be useful for both traditional high inertia and future low inertia systems, it is clear that with the reduction in inertial reserve the allowable delay gains immense significance. For example, an autorecloser can contain and extinguish temporary faults and protect the rest of the power system from the faulted section, but the fault-clearing operation may require several hundreds of milliseconds. The load-generation imbalance induced by the duration of such auto-reclosing operation in a low inertia system may trigger a frequency excursion event.

Besides, loads can also get disconnected during voltage sag events triggered by faults. Because a majority of loads and generators within a low-inertia system are converter-interfaced, they need to be specifically designed to have low-voltage ride-through capability. To counter these events, sufficient reserve needs to be allocated to protect the system from frequency contingencies. The calculation of reserve requirement to protect the power system from temporary faults will be considered in future work.

VI. CONCLUSION

A heuristic expression together with analytical and numerical verification of the delay margin for the deadbeat response and the small-signal marginal stability condition has been proposed in this paper for an approximated retarded low-inertia power

system. The expression is obtained by approximating the delay function using a Padé approximation. It has been shown that the first-order approximation for the deadbeat response and the second-order approximation for the marginal stability condition generally lead to better accuracy because the overall system gain of the approximated system falls below -3.01 dB of the DC gain of the system at the defined cut-off frequency. The proposed heuristic will be mainly useful for market operators in the reserve market of future power systems to alleviate the causality dilemma, wherein the maximum allowable delay is required to economically clear a successful bidding generator. It has also been shown that if the regulation factor of each of the reserve providing generators is selected based on their bid, and the response of the generators is fast enough compared to the heuristic presented, the generators can stabilize the whole system using droop control without violating their capacity limits. While it is impractical that all the generators would simultaneously respond at the maximum allowable time delay, ensuring that the slowest generator conforms to the maximum allowable delay supersedes the desired frequency response of the power system.

REFERENCES

[1] A. Ulbig, T. S. Borsche, and G. Andersson, "Impact of low rotational inertia on power system stability and operation," *IFAC Proc. Vol.*, vol. 47, no. 3, pp. 7290–7297, Aug. 2014.

[2] H. Thiesen, C. Jauch, and A. Gloe, "Design of a system substituting today's inherent inertia in the European continental synchronous area," *Energies*, vol. 9, no. 8, Apr. 2016, Art. no. 582.

[3] P. Tielens and D. Van Hertem, "Grid inertia and frequency control in power systems with high penetration of renewables," in *Proc. Young Researchers Symp. Elect. Power Eng.*, Delft, The Netherlands, Jun. 2012, pp. 1–6.

[4] B. Kroposki *et al.*, "Achieving a 100% renewable grid: Operating electric power systems with extremely high levels of variable renewable energy," *IEEE Power Energy Mag.*, vol. 15, no. 2, pp. 61–73, Mar. 2017.

[5] O. I. Elgerd, *Electric Energy Systems Theory: An Introduction*. New York, NY, USA: McGraw-Hill, 1982.

[6] N. Soni, S. Doolla, and M. C. Chandorkar, "Improvement of transient response in microgrids using virtual inertia," *IEEE Trans. Power Del.*, vol. 28, no. 3, pp. 1830–1838, Jun. 2013.

[7] P. Tielens and D. V. Hertem, "The relevance of inertia in power systems," *Renewable Sustain. Energy Rev.*, vol. 55, pp. 999–1009, 2016.

[8] N. Miller *et al.*, "Technology capabilities for fast frequency response," GE Energy Consulting, Boston, MA, USA, Tech. Rep., Mar. 2017. [Online]. Available: https://www.aemo.com.au/-/media/Files/Electricity/NEM/Security_and_Reliability/Reports/2017/2017-03-10-GE-FFR-Advisory-Report-Final---2017-3-9.pdf

[9] B. Chaudhuri, R. Majumder, and B. C. Pal, "Wide-area measurement-based stabilizing control of power system considering signal transmission delay," *IEEE Trans. Power Syst.*, vol. 19, no. 4, pp. 1971–1979, Nov. 2004.

[10] X. Xie, Y. Xin, J. Xiao, J. Wu, and Y. Han, "WAMS applications in Chinese power systems," *IEEE Power Energy Mag.*, vol. 4, no. 1, pp. 54–63, Jan. 2006.

[11] C. Hultholm and N. Wägar, "Optimal reserve operation in Turkey—Frequency control and non-spinning reserves," Wärtsilä, Helsinki, Finland, Tech. Rep., 2015. [Online]. Available: https://cdn.wartsila.com/docs/default-source/power-plants-documents/events/optimal-reserve-operation-in-turkey---frequency-control-and-non-spinning-reserves.pdf

[12] H. Jia, N. Guangyu, S. T. Lee, and P. Zhang, "Study on the impact of time delay to power system small signal stability," in *Proc. IEEE Mediterranean Electrotech. Conf.*, May 2006, pp. 1011–1014.

[13] Ş. Sönmez, S. Ayasun, and C. O. Nwankpa, "An exact method for computing delay margin for stability of load frequency control systems with constant communication delays," *IEEE Trans. Power Syst.*, vol. 31, no. 1, pp. 370–377, Jan. 2016.

[14] H. Jia, X. Cao, X. Yu, and P. Zhang, "A simple approach to determine power system delay margin," in *Proc. IEEE Power Eng. Soc. General Meeting*, Jun. 2007, pp. 1–7.

[15] Ş. Sönmez, S. Ayasun, and U. EmiŠnoğlu, "Computation of time delay margins for stability of a single-area load frequency control system with communication delays," *WSEAS Trans. Power Syst.*, vol. 9, pp. 67–76, 2014.

[16] K. Walton and J. E. Marshall, "Direct method for TDS stability analysis," *IEE Proc. D-Control Theory Appl.*, vol. 134, no. 2, pp. 101–107, Mar. 1987.

[17] P. Fu, S. I. Niculescu, and J. Chen, "Stability of linear neutral time-delay systems: Exact conditions via matrix pencil solutions," in *Proc. Amer. Control Conf.*, Jun. 2005, vol. 6, pp. 4259–4264.

[18] J.-H. Su, "The asymptotic stability of linear autonomous systems with commensurate time delays," *IEEE Trans. Autom. Control*, vol. 40, no. 6, pp. 1114–1117, Jun. 1995.

[19] F. Milano and M. Anghel, "Impact of time delays on power system stability," *IEEE Trans. Circuits Syst. I, Reg. Papers*, vol. 59, no. 4, pp. 889–900, Apr. 2012.

[20] J. M. Thangaiah and R. Parthasarathy, "Delay-dependent stability analysis of power system considering communication delays," *Int. Trans. Elect. Energy Syst.*, vol. 27, no. 3, 2017, Art. no. e2260.

[21] C. Dong *et al.*, "Effective method to determine time-delay stability margin and its application to power systems," *IET Gener. Transmiss. Distrib.*, vol. 11, no. 7, pp. 1661–1670, 2017.

[22] A. Ramírez, M. H. Koh, and R. Sipahi, "An approach to compute and design the delay margin of a large-scale matrix delay equation," *Int. J. Robust Nonlinear Control*, vol. 29, pp. 1101–1121, 2019.

[23] A. Khalil and A. Swee Peng, "An accurate method for delay margin computation for power system stability," *Energies*, vol. 11, no. 12, 2018, Art. no. 3466.

[24] G. A. Baker and P. R. Graves-Morris, *Padé Approximants: Basic Theory* (Encyclopedia of Mathematics and Its Applications). Reading, MA, USA: Addison-Wesley, 1981.

[25] C. Moler and C. Van Loan, "Nineteen dubious ways to compute the exponential of a matrix, twenty-five years later," *SIAM Rev.*, vol. 45, no. 1, pp. 3–49, Feb. 2003.

[26] M. Vajta, "Some remarks on Padé-approximations," in *Proc. 3rd TEMPUS-INTCOM Symp. Intell. Syst. Control Meas.*, Sep. 2000, pp. 1–6.

[27] F. Milano, "Small-signal stability analysis of large power systems with inclusion of multiple delays," *IEEE Trans. Power Syst.*, vol. 31, no. 4, pp. 3257–3266, Jul. 2016.

[28] S. A. Pourmousavi and M. H. Nehrir, "Introducing dynamic demand response in the LFC model," *IEEE Trans. Power Syst.*, vol. 29, no. 4, pp. 1562–1572, Jul. 2014.

[29] M. F. M. Arani and Y. A. I. Mohamed, "Cooperative control of wind power generator and electric vehicles for microgrid primary frequency regulation," *IEEE Trans. Smart Grid*, vol. 9, no. 6, pp. 5677–5686, Nov. 2018.

[30] F. Yang, J. He, and D. Wang, "New stability criteria of delayed load frequency control systems via infinite-series-based inequality," *IEEE Trans. Ind. Inform.*, vol. 14, no. 1, pp. 231–240, Jan. 2018.

[31] Y. G. Rebours, D. S. Kirschen, M. Trotignon, and S. Rossignol, "A survey of frequency and voltage control ancillary services—Part II: Economic features," *IEEE Trans. Power Syst.*, vol. 22, no. 1, pp. 358–366, Feb. 2007.

[32] J. Morren, S. W. H. de Haan, and J. A. Ferreira, "Contribution of DG units to primary frequency control," *Euro. Trans. Electr. Power*, vol. 16, pp. 507–521, Sep. 2006.

[33] J. Fleer *et al.*, "Price development and bidding strategies for battery energy storage systems on the primary control reserve market," in *Proc. 11th Int. Renewable Energy Storage Conf.*, Düsseldorf, Germany, Mar. 2017, pp. 143–157.

[34] T. Borsche, A. Ulbig, M. Koller, and G. Andersson, "Power and energy capacity requirements of storages providing frequency control reserves," in *Proc. IEEE Power Energy Soc. General Meeting*, Jul. 2013, pp. 1–5.

[35] D. Soler, P. Frias, T. Gomez, and C. A. Platero, "Calculation of the elastic demand curve for a day-ahead secondary reserve market," *IEEE Trans. Power Syst.*, vol. 25, no. 2, pp. 615–623, May 2010.

[36] A. Molina-Garcia, F. Bouffard, and D. S. Kirschen, "Decentralized demand-side contribution to primary frequency control," *IEEE Trans. Power Syst.*, vol. 26, no. 1, pp. 411–419, May 2011.

[37] X. Luo, J. Wang, M. Dooner, and J. Clarke, "Overview of current development in electrical energy storage technologies and the application potential in power system operation," *Appl. Energy*, vol. 137, pp. 511–536, 2015.

[38] K. Ogata and Y. Yang, *Modern Control Engineering*. Delhi, India: Prentice Hall India, 2002.

[39] J. Rommes and N. Martins, "Efficient computation of transfer function dominant poles using subspace acceleration," *IEEE Trans. Power Syst.*, vol. 21, no. 3, pp. 1218–1226, Aug. 2006.

Shrikrishna A. Khaparde (SM'91) received the Ph.D. degree from the Indian Institute of Technology Kharagpur, Kharagpur, India, in 1981.

He is currently a Professor with the Department of Electrical Engineering, Indian Institute of Technology Bombay, Mumbai, India. His current research areas are smart grids, distributed generation, renewable energy policies, restructured power systems, and CIM implementation in India.

Sarath Perera (SM'12) received the Ph.D. degree from the University of Wollongong, Wollongong, NSW, Australia, in 1988.

He is currently a Professor and the Technical Director with the Australian Power Quality and Reliability Centre, University of Wollongong.

Subir Majumder (S'17) is currently working toward the Ph.D. degree under the joint Ph.D. program between the Indian Institute of Technology Bombay, Mumbai, India and University of Wollongong, Wollongong, NSW, Australia.

His research interests include power systems modeling, operations and planning, power system economics, and the smart grid.

S. V. Kulkarni (SM'08–F'19) received the Ph.D. degree from the Indian Institute of Technology Bombay, Mumbai, India, in 2000.

He is currently a Professor with the Electrical Engineering Department, Indian Institute of Technology Bombay. His research interests include analysis and diagnostics of power transformers, computational electromagnetics, distributed generation and smart grids.

Ashish Prakash Agalgaonkar (SM'13) received the Ph.D. degree from the Indian Institute of Technology Bombay, Mumbai, India, in 2006.

He is currently a Senior Lecturer with the University of Wollongong, Wollongong, NSW, Australia. His research interests include planning and operational aspects of renewable and distributed generation, power system reliability, microgrids, electricity markets, and system stability.

Philip Paul Ciufo (SM'07) received the Ph.D. degree in electrical engineering from the University of Wollongong, Wollongong, NSW, Australia, in 2002.

He was an Associate Professor with the University of Wollongong. His research interests included ac machines, advanced distribution system automation, and power quality.